

Supporting Information

Highly Selective Dual-Modal Probe for Photoacoustic and Magnetic

Resonance Imaging of Labile Cu²⁺ Pool in the Liver

Zhaoqing Liu^{a, b, #}, Lei Zhang^{a, b, #}, Sha Li^{a, b}, Long Xiao^{a, b}, Qiao Yu^a, Yue Zhu^a, Yingying Luo^{a, b}, Maosong Qiu^{a, b}, Xin Zhou^{a, b, c}, Shizhen Chen^{a, b, c*}

^a State Key Laboratory of Magnetic Resonance Spectroscopy and Imaging, National Center for Magnetic Resonance in Wuhan, Wuhan Institute of Physics and Mathematics, Innovation Academy for Precision Measurement Science and Technology, Chinese Academy of Sciences, Wuhan, 430071, P. R. China.

^b University of Chinese Academy of Sciences, Beijing, 100049, P. R. China.

^c School of Biomedical Engineering, Hainan University, Sanya 572019, P. R. China.

* Corresponding author: chenshizhen@wipm.ac.cn.

These authors contributed equally to this work.

Table of Contents

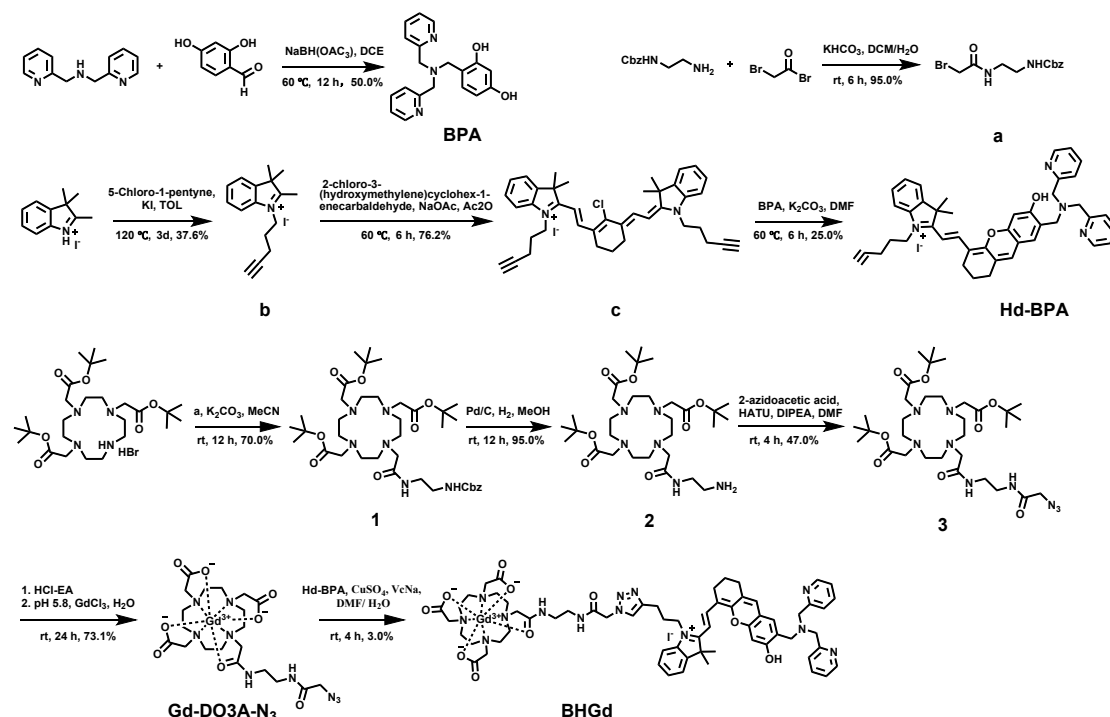
1. Materials and instruments.....	S3
2. Chemical Synthesis of Compounds.....	S3
3. Cell Culture Conditions.....	S6
4. Cell Viability Assays.....	S6
5. Fluorescence Imaging of Cells.....	S6
6. Flow Cytometry.....	S6
7. Animals.....	S6
8. Toxicity Assessment.....	S7
9. Figures.....	S8
10. ¹ H NMR and HRMS spectra	S17

S1. Materials and Instruments

Bis(pyridin-2-ylmethyl)amine, 2,4-dihydroxybenzaldehyde, 1,4,7,10-tetraazacyclododecane, 2,3,3-Trimethylindolenine, Tetrabutylammonium bromide, and Benzyl N-(2-aminoethyl)carbamate hydrochloride, 5-Chloro-1-pentyne, O-(7-Azabenzotriazol-1-yl)-N,N,N',N'-tetramethyl uranium hexafluorophosphate, N'1,N'3-Dimethyl-N'1,N'3-di(phenylcarbonothioyl)malonohydrazide (Elesclomol, TETA), Sodium triacetoxymethylborohydride, 2-Hydroxy-N,N,N-trimethylethanaminium tetrathiomolybdate (ATN-224), Gadolinium(III) chloride hexahydrate and 2-Chloro-3-(hydroxymethylene)cyclohex-1-enecarbaldehyde were purchased from Shanghai Bide Pharmaceutical Co., Ltd. T-butyl 2-bromoacetate, Sodium borohydride, 2-azidoacetic acid, N,N-Diisopropylethylamine, 10% Pd/C and 2-bromoacetyl bromide were purchased from Discovery Technology Co., Ltd. Concentrated hydrochloric acid, Sodium hydroxide, Potassium carbonate, Sodium acetate, Potassium bicarbonate, Potassium iodide, Cupric sulfate, Magnesium sulfate, Zinc chloride, Ferric chloride, Calcium chloride, Sodium ascorbate and other solvents were purchased from Chinese Pharmaceutical Co., Ltd. $[\text{Cu}(\text{NCCH}_3)_4]\text{PF}_6$ was purchased from Aladdin. Human serum albumin (HSA) was purchased from Aladdin. The 200 - 300 mesh TLC silica-gel powder was purchased from Qingdao Foreign Chemical Industry Co., Ltd. MCF-10A cells were obtained from Cell Bank of the Chinese Academy of Sciences (Shanghai, China). BALB/c nude mice were purchased from Wuhan Bainte Biotechnology Co., Ltd. Pure and ultrapure water were prepared and purified using a Milli-Q reference system (Millipore).

The ^1H NMR spectra were acquired on a 500 MHz Bruker spectrometer. High-performance liquid chromatography (HPLC) was carried out on Shimadzu LC-20A using $\text{CH}_3\text{CN}/\text{H}_2\text{O}$ (0.1% CF_3COOH) as the eluent. High-resolution mass spectra (HRMS) were recorded on a Bruker micro-TOF-QII mass spectrometer with electrospray ionization (ESI). UV-vis spectra were recorded on an Evolution-220 UV-vis spectrometer (Thermo Scientific, USA). Fluorescence spectra were measured with an Edinburgh FS5 fluorescence spectrometer equipped with a 150 W xenon lamp. MR relaxivity was acquired on a 20 MHz MR relaxometer (Niumag, China), and *in vitro* and *in vivo* MR imaging experiments were conducted on a 9.4 T MR scanner (Bruker, Germany). Fluorescent images of cells were acquired with a fluorescence microscope (Nikon, Japan). MTT assay was performed on a microplate reader (Spectra Max 190). All photoacoustic (PA) imaging experiments were performed on a multispectral optoacoustic tomographic system (MOST, Germany).

S2. Chemical Synthesis of Compounds



Scheme S1. Synthetic pathway of **BHGd**.

Synthesis of compound **BPA**

A solution of bis(pyridin-2-ylmethyl)amine (5.0 g, 25.0 mmol) and 2,4-dihydroxybenzaldehyde (7.0 g, 50.2 mmol) in dichloromethane (DCM, 150 mL) was stirred at 60 °C under a nitrogen atmosphere for 3 hours. After cooling to room temperature, sodium triacetoxyborohydride (10.6 g, 50.2 mmol) was added portionwise. The reaction was stirred at room temperature overnight. The solution was transferred to a separatory funnel, and the aqueous layer was extracted with DCM (3 × 100 mL). The combined organic layers were dried over anhydrous Na₂SO₄ and concentrated. The residue was purified by column chromatography on silica gel (DCM/MeOH = 95:5) to afford the product **BPA** (4.0 g, 50%) as a white solid. ¹H NMR (500 MHz, CDCl₃) δ 8.55 (d, *J* = 4.5 Hz, 2H), 7.61 (t, *J* = 7.5 Hz, 2H), 7.35 (d, *J* = 5 Hz, 2H), 7.26 (s), 7.15 (t, *J* = 6.3 Hz, 2H), 6.86 (d, *J* = 8.0 Hz, 1H), 6.45 (d, *J* = 2.0 Hz, 1H), 6.27 (dd, *J* = 8.1, 2.3 Hz, 1H), 3.86 (s, 4H), 3.69 (s, 2H) (Figure S21). HRMS (ESI) Calcd for C₁₉H₁₉N₃O₂, [M+H]⁺: 322.1477, Found: 322.1506 (Figure S22).

Synthesis of compound **Hd-BPA**

The compounds **b** and **c** were synthesized according to literature procedures.¹ To a solution of compound **BPA** (2.2 g, 6.8 mmol) and potassium carbonate (939.8 mg, 6.8 mmol) in DMF (50 mL), a solution of compound **c** (2.0 g, 2.8 mmol) in DMF (10 mL) was added under a nitrogen atmosphere. The reaction was stirred at 70 °C for 12 h. The reaction mixture was cooled to room temperature and filtered to remove potassium carbonate. The solvent was then evaporated in vacuo. A mixture solution of H₂O (200 mL) and DCM (250 mL) was added, and the two phases were separated. The aqueous layer was extracted with DCM (3 × 50 mL). The combined organic layers were dried over anhydrous Na₂SO₄ and concentrated. The residue was purified by chromatography on silica gel column (DCM/MeOH = 94:6) to afford the product **Hd-BPA** (541.96 mg, 25.0%) as a blue solid. ¹H NMR (500 MHz, CDCl₃) δ 8.79 (dd, *J* = 5.0 Hz, 2H), 8.59 (dd, *J* = 15.0 Hz, 1H), 8.25 (s, 2H),

7.98 (d, $J = 10.0$ Hz, 2H), 7.67 (s, 2H), 7.42 – 7.36 (m, 2H), 7.31 – 7.28 (m, 2H), 7.23 (d, $J = 20$ Hz, 2H), 7.19 (s) 6.94 (s, 1H), 6.21 (dd, $J = 15.0$ Hz, 1H), 4.27 (s, 4H), 4.22 (d, $J = 5$ Hz, 2H), 3.72 (s, 2H), 2.67 (dd, $J = 56.2$ Hz, 4H), 2.32 (dd, 2H), 2.11 (s, 1H), 2.01 (d, $J = 15.0$ Hz, 2H), 1.83 (s, 2H), 1.69 (s, 6H). ^{13}C NMR (126 MHz, CDCl_3) δ 176.49, 163.34, 161.74, 161.41, 161.11, 160.81, 160.51, 154.76, 153.68, 145.60, 145.34, 142.41, 141.52, 141.28, 136.87, 131.23, 129.02, 127.08, 126.84, 126.26, 125.48, 122.79, 121.53, 119.53, 117.23, 114.91, 114.75, 112.62, 112.60, 111.29, 102.83, 101.26, 82.21, 77.30, 77.04, 76.79, 70.77, 56.41, 52.79, 50.36, 43.36, 28.69, 28.23, 25.99, 24.04, 20.27, 15.99, 14.13 (Figures S23 and S24). HRMS (ESI) Calcd for $\text{C}_{43}\text{H}_{43}\text{IN}_4\text{O}_3$, $[\text{M}-\text{I}]^+$: 647.8425, Found: 647.7856 (Figure S25).

Synthesis of compound 1

To a solution of Tri-tert-butyl 2,2',2''-(1,4,7,10-tetraazacyclododecane-1,4,7-triyl)triacetate hydrochloride (3.0 g, 5.0 mmol) and potassium carbonate (1.9 g, 13.9 mmol) in acetonitrile (CH_3CN , 150 mL), a solution of compound **a** (2.2 g, 7.0 mmol) in CH_3CN (100 mL) was added. The reaction was stirred at room temperature overnight. The CH_3CN was evaporated in vacuo, and the residue was purified by chromatography on silica gel column (DCM/MeOH = 100:3) to afford product **1** (2.6 g, 70.0%) as a white solid. ^1H NMR (500 MHz, CDCl_3): δ 7.29 (t, $J = 5.0$ Hz, 4H), 7.21 – 7.18 (t, $J = 15.0$ Hz, 1H), 5.06 (s, 2H), 3.42 – 3.31 (m, 9H), 2.97 – 2.01 (m, 19H), 1.45 (d, $J = 15.0$ Hz, 27H) (Figure S26). HRMS (ESI) Calcd for $\text{C}_{38}\text{H}_{64}\text{N}_6\text{O}_9$, $[\text{M}+\text{Na}]^+$: 771.4735, Found: 771.4639 (Figure S27).

Synthesis of compound 2

Compound **1** (1.0 g, 1.3 mmol) and Pd/C (100 mg, 10 wt %) were stirred in MeOH under 1 atm of $\text{H}_2(\text{g})$ overnight. The mixture was filtered to remove Pd/C, and the solid part was washed multiple times with DCM (20 mL). The filtrate was combined and concentrated to afford product **2** (779.6 mg, 95%) as a white solid. ^1H NMR (500 MHz, CDCl_3): δ 3.62 (s, 2H), 3.47 – 3.18 (m, 8H), 2.81 – 2.22 (m, 18H), 1.45 (s, 27H) (Figure S28). HRMS (ESI) Calcd for $\text{C}_{30}\text{H}_{58}\text{N}_6\text{O}_7$, $[\text{M}+\text{Na}]^+$: 637.4367, Found: 637.4480 (Figure S29).

Synthesis of compound 3

To a mixture of 2-azidoacetic acid (126.2 mg, 1.3 mmol) and HATU (475.0 mg, 1.3 mmol) in DMF (15 mL), a solution of DIPEA (201.8 mg, 1.6 mmol) and the compound **2** (640.0 mg, 1.0 mmol) in DMF (15 mL) was added. The reaction was stirred at room temperature for 4 h. The mixture was then evaporated in vacuo and extracted with DCM (100 mL) and H_2O (100 mL). The organic layer was dried over anhydrous Na_2SO_4 for 30 minutes and concentrated. The residue was purified by chromatography on silica gel column (DCM/MeOH = 100:3) to afford the product **3** (320.1 mg, 47.0%) as a white solid. ^1H NMR (500 MHz, CDCl_3) δ 8.00 (s, 2H), 7.28 (s, 1H), 5.29 (s, 1H), 3.86 (s, 2H), 3.64 (d, $J = 100.0$ Hz, 8H), 2.95 (s, 8H), 2.86 (s, 8H), 2.79 (s, 4H), 1.44 (d, $J = 6.2$ Hz, 27H) (Figure S30). HRMS (ESI) Calcd for $\text{C}_{32}\text{H}_{59}\text{N}_9\text{O}_8$, $[\text{M}+\text{Na}]^+$: 720.4487, Found: 720.4382 (Figure S31).

Synthesis of compound Gd-DO3A- N_3

A solution of compound **3** (300.0 mg, 430.0 μmol) in 4 M HCl-ethyl acetate (60 mL) was stirred at room temperature overnight. The HCl-ethyl acetate solution was removed by rotary evaporation

under reduced pressure, and the residue was dissolved in ultrapure water (30 mL). The pH of the solution was adjusted to 6.0. $\text{GdCl}_3 \cdot 6\text{H}_2\text{O}$ (226.7 mg, 0.86 mmol) in ultrapure water was added, and the mixture was stirred for 6 h. The mixture solution was concentrated in vacuo, the reaction mixture was purified by preparative RP-HPLC on a C18 column to afford product **Gd-DO3A-N₃**² (215.4 mg, 73.1%) as a white solid. HRMS (ESI) Calcd for $\text{C}_{20}\text{H}_{32}\text{GdN}_9\text{O}_8$, $[\text{M}+\text{H}]^+$: 685.1615, Found: 685.1623 (Figure S1).

S3. Cell Culture Conditions

MCF-10A cells were cultured in high-glucose Dulbecco's Modified Eagle Medium (DMEM, Cell-Box) supplemented with 10% fetal bovine serum (FBS) and 1% penicillin/streptomycin (PS). The cells were maintained in a humidified atmosphere of 5% CO_2 and 95% air at 37 °C.

S4. Cell Viability Assays

The cytotoxicity of **BHGd** to MCF-10A cells was evaluated by Cell Counting Kit-8 (CCK-8) Cell Proliferation and Cytotoxicity assay following the manufacturer's protocol. Briefly, MCF-10A cells (1×10^5 cells/well) in DMEM supplemented with 10% FBS (200 μL) were seeded in 96-well plates and incubated at 37 °C overnight. The medium was then replaced, and cells were treated with **BHGd** at a series of concentrations (0, 6.3, 12.5, 25, 50, 75, and 100 μM) in FBS-free DMEM (100 μL). The cells were incubated at 37 °C in a humidified atmosphere of 5% CO_2 and 95% air for 12 h or 24 h. After the removal of the medium, FBS-free DMEM (90 μL) supplemented with CCK-8 (10 μL , 1:100 dilution) was added to each well. The plates were incubated at 37 °C with 5% CO_2 and 95% humidity for 2 h. Absorbance at 450 nm was measured with a microplate reader and cell viability was calculated based on untreated wells. Data are presented as mean \pm SD ($n = 3$).

S5. Fluorescence Imaging of Cells

Cells were dispersed onto a glass-bottom dish (1×10^5 cells; Cellvis, D35-20-1-N, 35 mm dish with 20 mm bottom well) and allowed to grow for 24 h. For the uptake experiment, MCF-10A cells were incubated with **BHGd** (10 μM) in FBS-free DMEM at various time points (1 h, 2 h, 4 h, 6 h, 8 h, and 12 h). The culture medium was removed, and the cells were washed three times with PBS. Fluorescence images were captured with a fluorescence microscope (Nikon, Japan) with the Cy5.5 channel for excitation and emission.

S6. Flow Cytometry

MCF-10A cells (1×10^5 cells per sample) were incubated in a glass-bottom dish containing **BHGd** (10 μM) at 37 °C in a humidified atmosphere of 5% CO_2 and 95% air for 6 h. After washing with PBS, the cells were transferred to a microcentrifuge tube and resuspended in PBS (100 μL). The fluorescence of cell samples was analyzed with a flow cytometer (CytoFLEX S, Beckman Coulter; NovoCyte Advantec, ACEA Biosciences).

S7. Animals

All animal experimental protocols were approved by the Animal Welfare and Research Ethics Committee at the Innovation Academy for Precision Measurement Science and Technology, CAS (APM23024T). BALB/c mice (4 - 6 weeks) were purchased from the Wuhan Bainte Biotechnology

Co., Ltd. Mice were housed at 25 °C with free access to food and water.

S8. Toxicity Assessment

BALB/c mice were intravenously injected with PBS (as control group, 0.5 M, 100 µL), **BHGd** (500 µM, 100 µL), and **BHGd** (500 µM, 100 µL) plus ATN-224 (5 mg/kg in 50 µL), respectively. For the acute toxicity, hematoxylin and eosin (H&E) staining analysis of major organs (heart, kidney, liver, lung and spleen) with different treatments was performed at 24 h post-injection.

S9 Figures

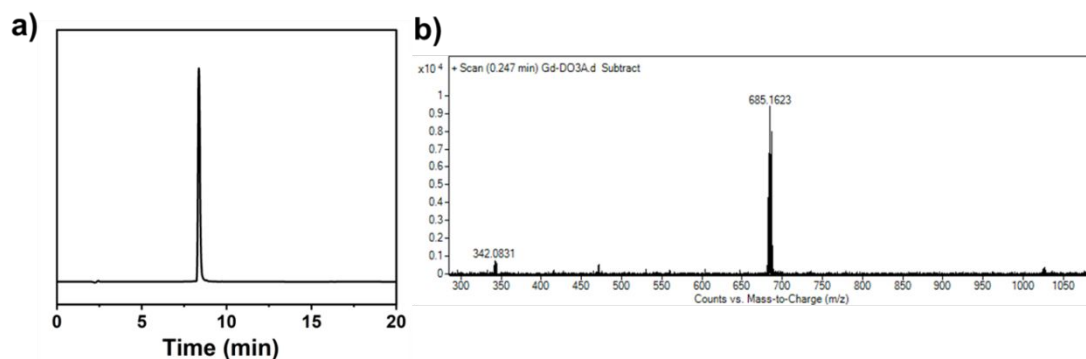


Figure S1. (a) HPLC and (b) mass spectra for compound **Gd-DO3A-N₃**.

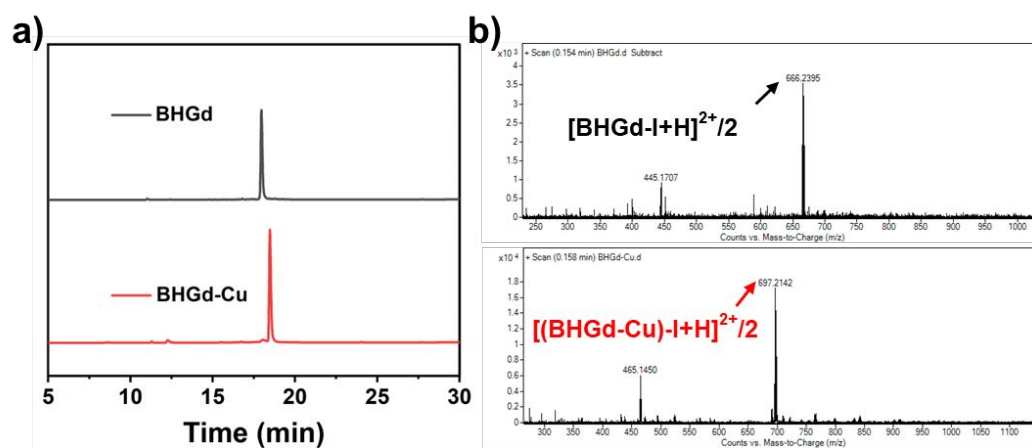


Figure S2. (a) HPLC and (b) mass spectra for **BHGd** and **BHGd-Cu**.

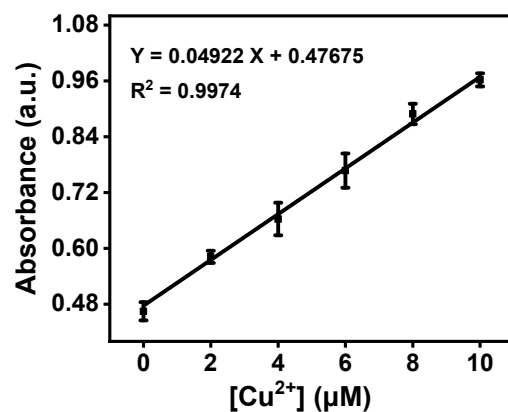


Figure S3. The linear fitting curve of UV intensity with the concentration of Cu^{2+} from 0 ~ 10 μM . The detection limit was found to be 0.15 μM , using a $3\sigma/k$ method.

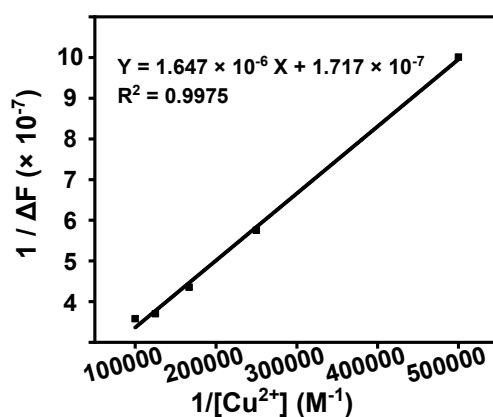


Figure S4. Benesi-Hildbr and equation plot of 10 μM **BHGd** with Cu^{2+} was obtained from fluorescence titration data. The binding constant was determined to be $1.04 \times 10^5 \text{ M}^{-1}$.

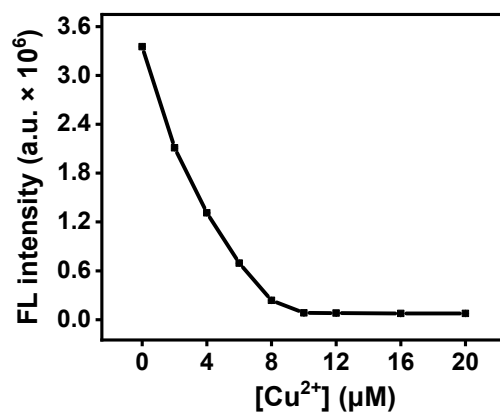


Figure S5. The fluorescence changes of **BHGd** (10 μM) upon treatment with Cu^{2+} (0 to 20 μM) at an excitation wavelength of 680 nm (0.1 M HEPES buffer, pH 7.4).

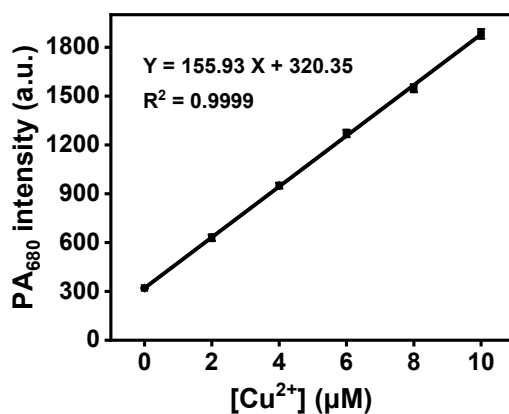


Figure S6. The linear fitting curve of PA intensity ($\lambda_{\text{ex}} = 680 \text{ nm}$) with the concentration of Cu^{2+} from 0 ~ 10 μM . The detection limit was found to be 0.11 μM , using a $3\sigma/k$ method.

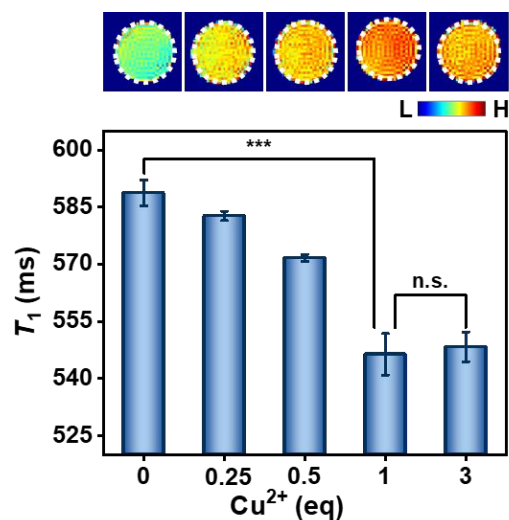


Figure S7. T_1 mapping images (top) and corresponding T_1 values (bottom) of **BHGd** (0.3 mM) with varying molar concentrations of Cu^{2+} (9.4 T, 0.1 M HEPES buffer at pH 7.4). Data are presented as mean \pm SD ($n = 3$), *** $P < 0.001$ and n.s., $P > 0.05$.

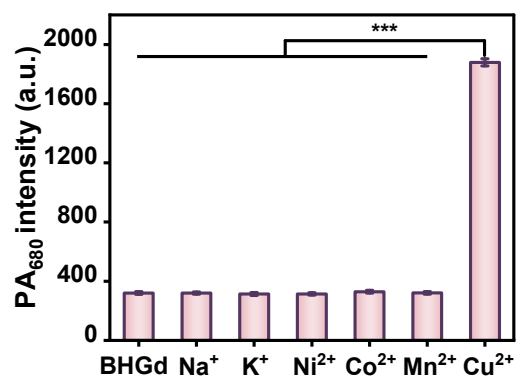


Figure S8. (a) Quantitative PA imaging analysis of **BHGd** (10 μM) in the presence of equimolar concentration of metal ions. Data are presented as mean \pm SD ($n = 3$), *** $P < 0.001$ and n.s., $P > 0.05$.

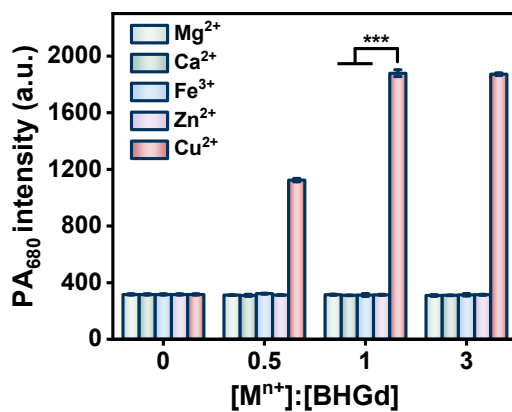


Figure S9. PA signal of **BHGd** 0.1 M HEPES buffer (10 μM) with varying concentrations of metal

ions (pH 7.4). Data are presented as mean \pm SD ($n = 3$), *** $P < 0.001$ and n.s., $P > 0.05$.

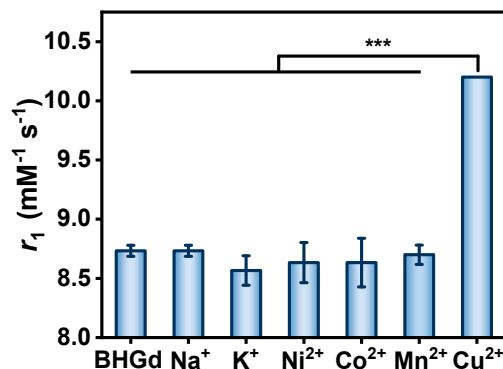


Figure S10. The r_1 of **BHGd** in the presence of equimolar metal ions. Data are presented as mean \pm SD ($n = 3$), *** $P < 0.001$ and n.s., $P > 0.05$.

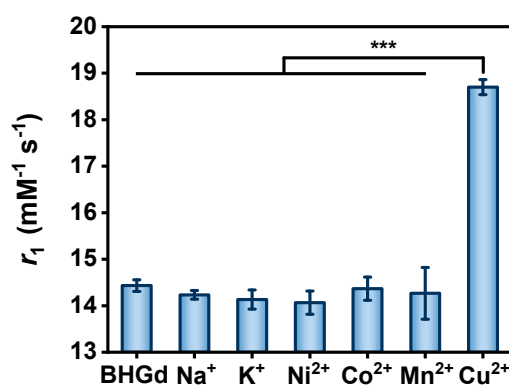


Figure S11. The r_1 of **BHGd** with equimolar metal ions in the presence of 0.6 mM HSA. Data are presented as mean \pm SD ($n = 3$), *** $P < 0.001$ and n.s., $P > 0.05$.

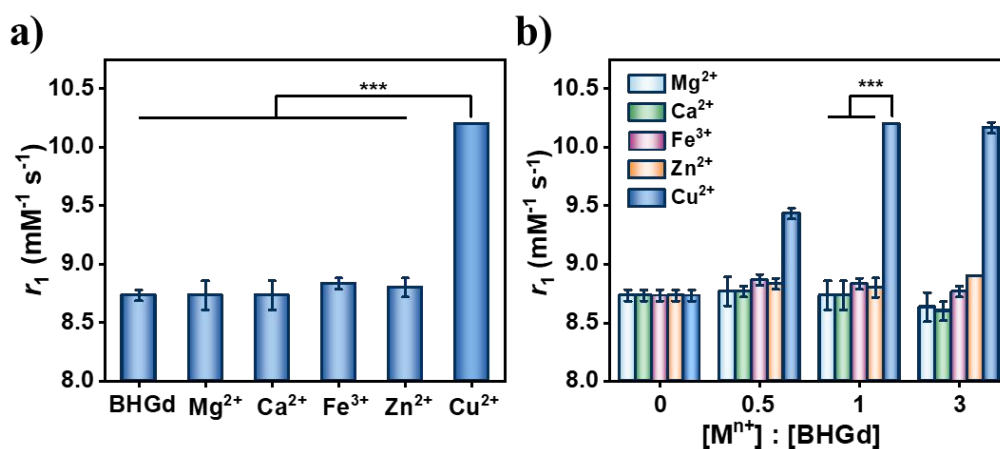


Figure S12. (a) The r_1 of **BHGd** with equimolar concentrations of metal ions. (b) The r_1 of **BHGd** with varying concentrations of metal ions acquired at 20 MHz and 37 °C. Data are presented as

mean \pm SD ($n = 3$), *** $P < 0.001$ and n.s., $P > 0.05$.

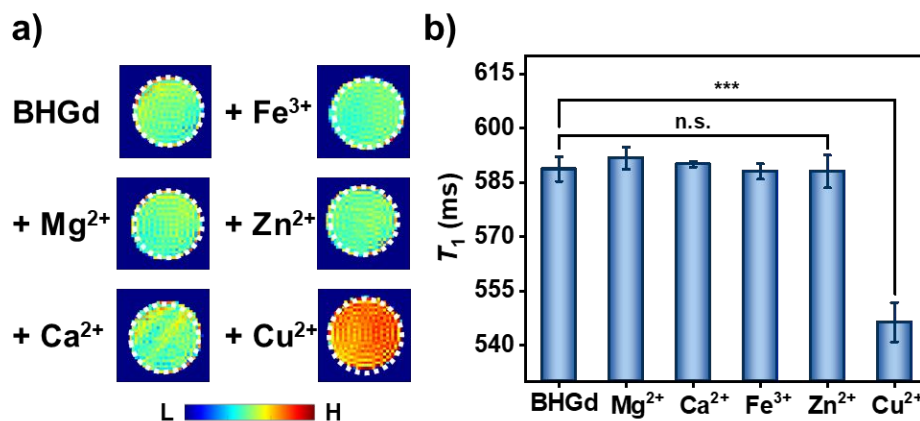


Figure S13. (a) T_1 mapping images and (b) corresponding T_1 values of phantoms containing **BHGd** (0.3 mM) with equimolar concentrations of metal ions. Data are presented as mean \pm SD ($n = 3$), *** $P < 0.001$ and n.s., $P > 0.05$.

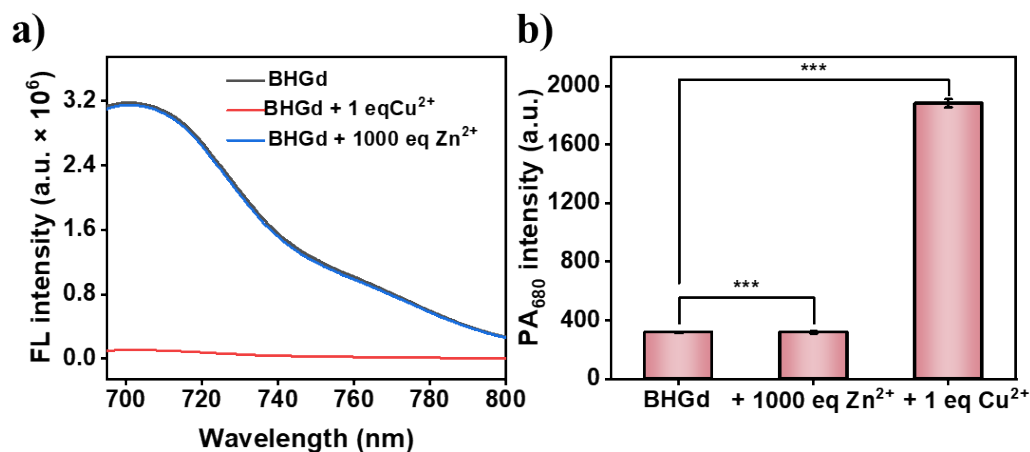


Figure S14. (a) Fluorescence spectra and (b) PA intensity of **BHGd** (10 μ M), **BHGd** in the presence of 1000 equivalents of Zn²⁺, and **BHGd** with 1 equivalent of Cu²⁺. Data are presented as mean \pm SD ($n = 3$), *** $P < 0.001$ and n.s., $P > 0.05$.

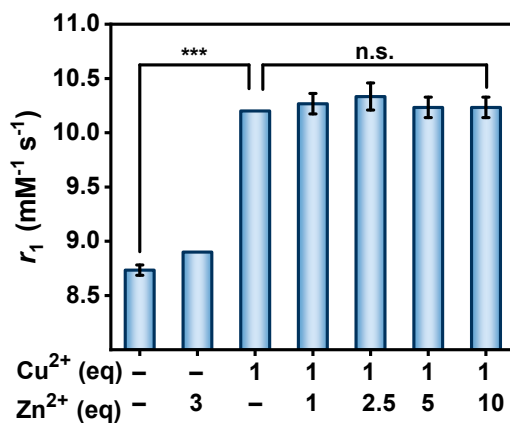


Figure S15. The r_1 of **BHGd** acquired at 20 MHz in 0.1 M HEPES buffer with Cu^{2+} in the presence of various concentrations of Zn^{2+} ions (1, 2.5, 5, and 10 equivalents). Data are presented as mean \pm SD ($n = 3$), *** $P < 0.001$ and n.s., $P > 0.05$.

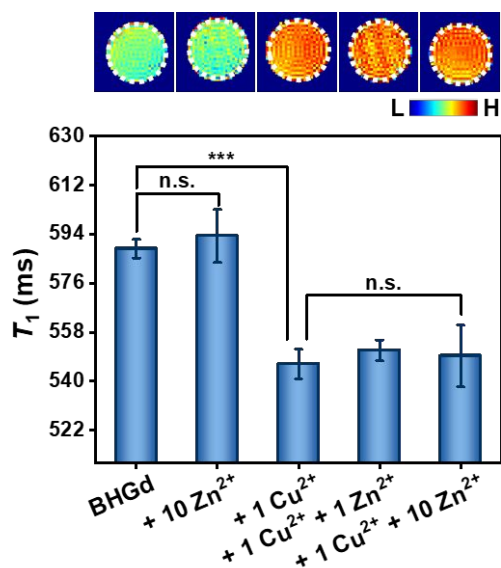


Figure S16. T_1 mapping images (top) and corresponding T_1 values (bottom) of phantoms were acquired at 9.4 T for **BHGd** (0.3 mM) in the presence of 0.6 mM HSA and various concentrations of Zn^{2+} (1 and 10 equivalents). Values are mean \pm SD ($n = 3$), Data are presented as mean \pm SD ($n = 3$), *** $P < 0.001$ and n.s., $P > 0.05$.

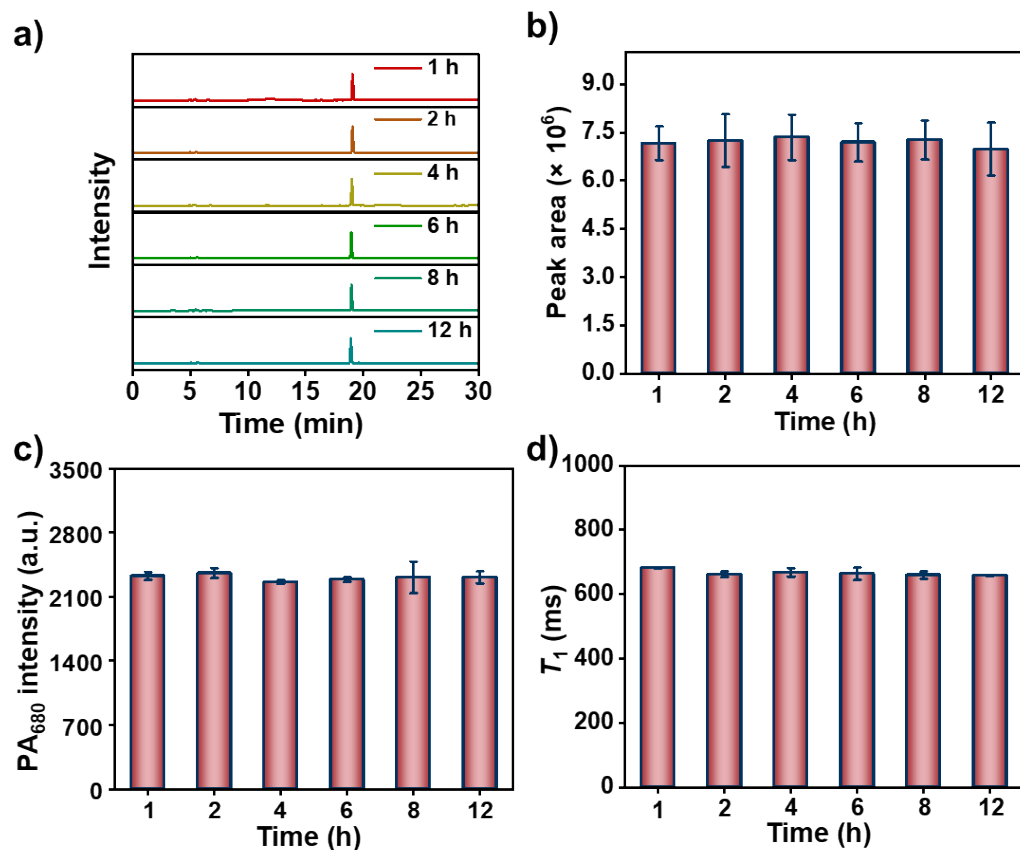


Figure S17. Stability test of **BHGd**. Time-dependent (a) HPLC traces, (b) HPLC peak area ratio, (c) PA intensity and (d) T_1 values of **BHGd** incubated in DMEM containing 10% FBS over different time points.

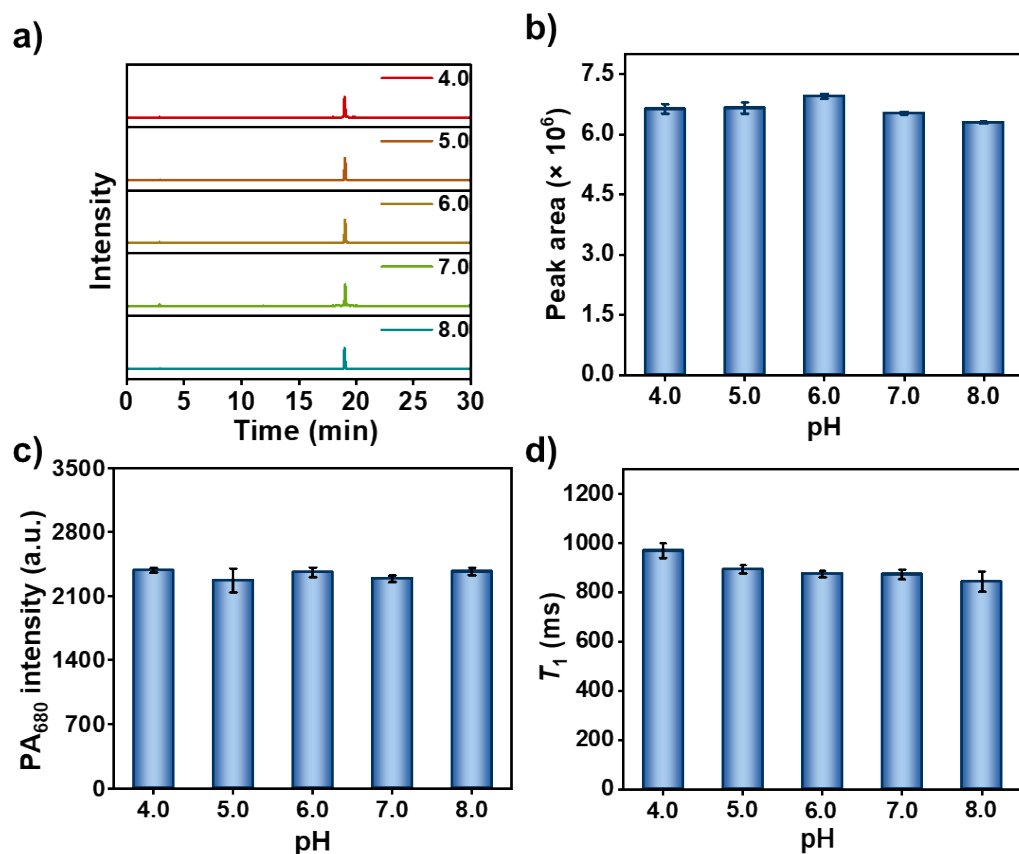


Figure S18. Stability test of **BHGd**. (a) HPLC traces, (b) HPLC peak area ratio, (c) PA intensity (excitation at 680 nm) and (d) T_1 values of **BHGd** incubated at different pH values for 6 h.

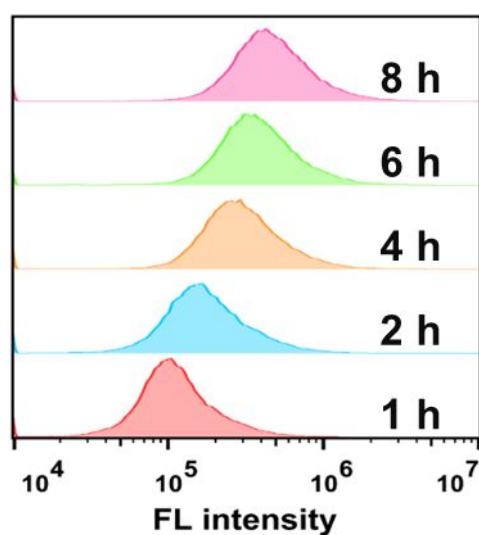


Figure S19. Flow cytometry analysis of MCF-10A cells incubated with **BHGd** (10 μ M) at 37 $^{\circ}$ C for 1 – 8 h.

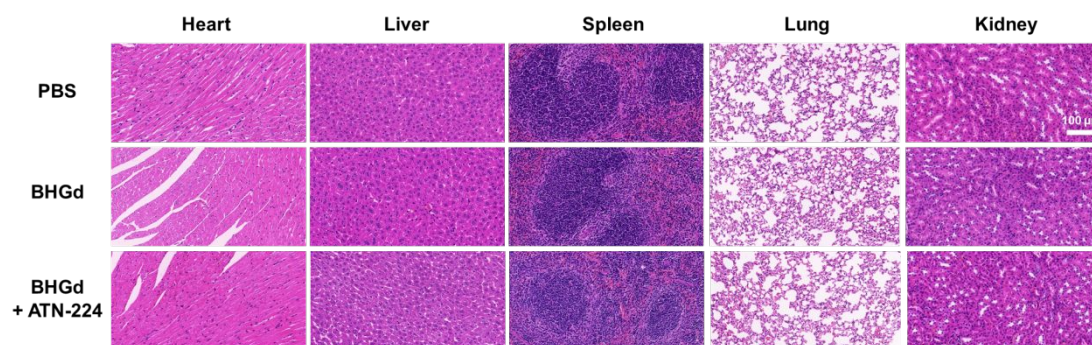


Figure S20. Hematoxylin and eosin (H&E) staining of tissue sections from mice intravenously with PBS, **BHGd**, and **BHGd** plus ATN-224 (Scale bar, 100 μ m).

References

- (1) Hyun, J. Y.; Kang, N. R.; Shin, I. Carbohydrate Microarrays Containing Glycosylated Fluorescent Probes for Assessment of Glycosidase Activities. *Org. Lett.* **2018**, *20* (4), 1240-1243.
- (2) Yu, Q.; Zhang, L.; Jiang, M.; Xiao, L.; Xiang, Y.; Wang, R.; Liu, Z.; Zhou, R.; Yang, M.; Li, C.; Liu, M.; Zhou, X.; Chen, S. An NIR Fluorescence Turn-on and MRI Bimodal Probe for Concurrent Real-time *in vivo* Sensing and Labeling of β -Galactosidase. *Angew. Chem., Int. Ed.* **2023**, *62* (46), e202313137.

S10. NMR and MS spectra

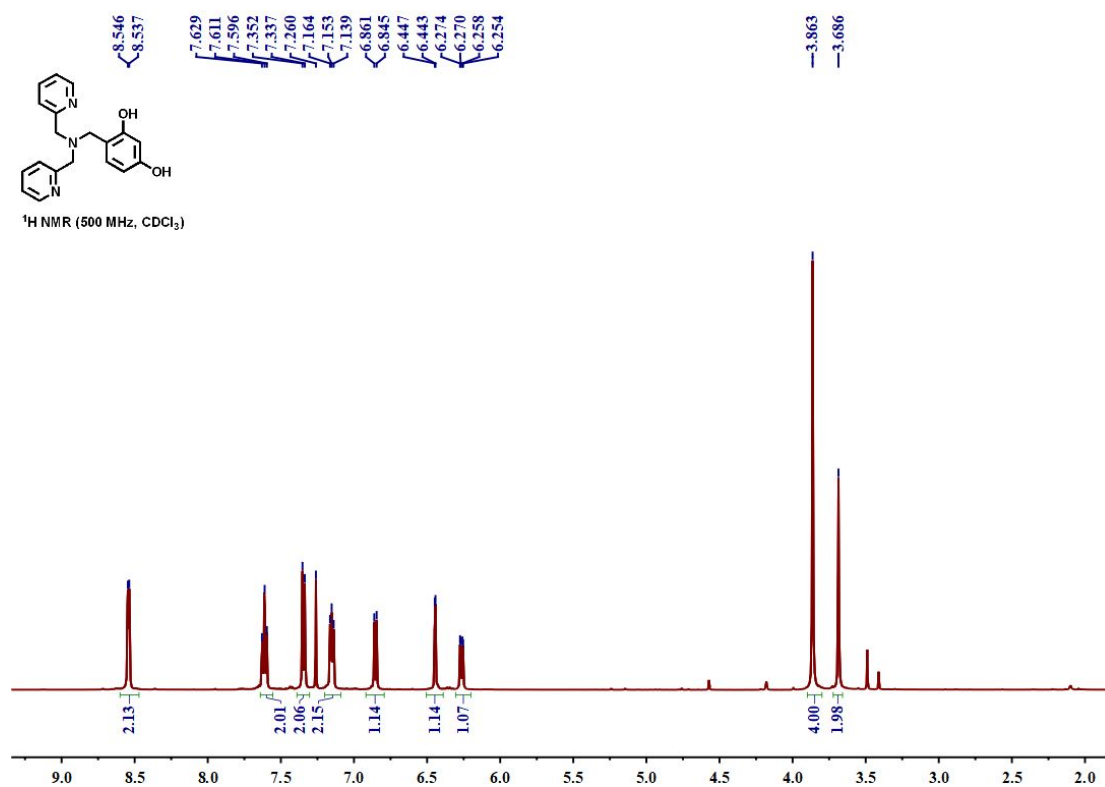


Figure S21. ^1H NMR spectrum of compound BPA in CDCl_3 .

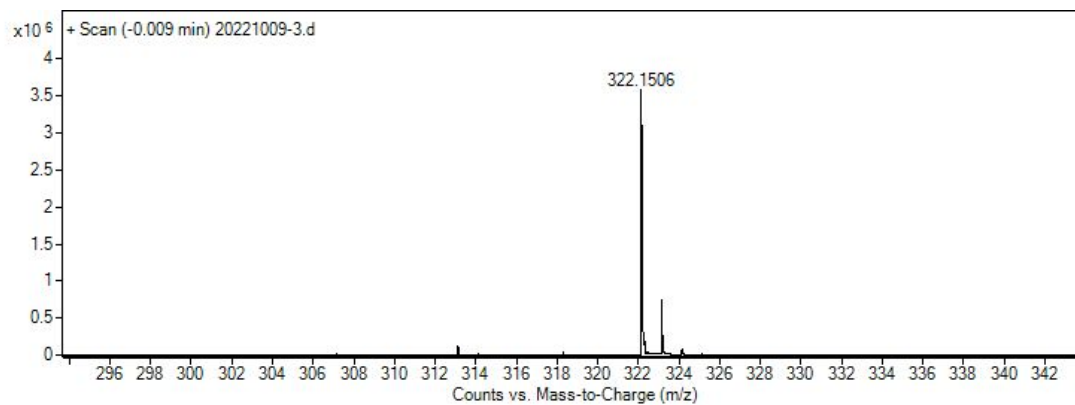


Figure S22. HRMS spectrum of compound BPA.

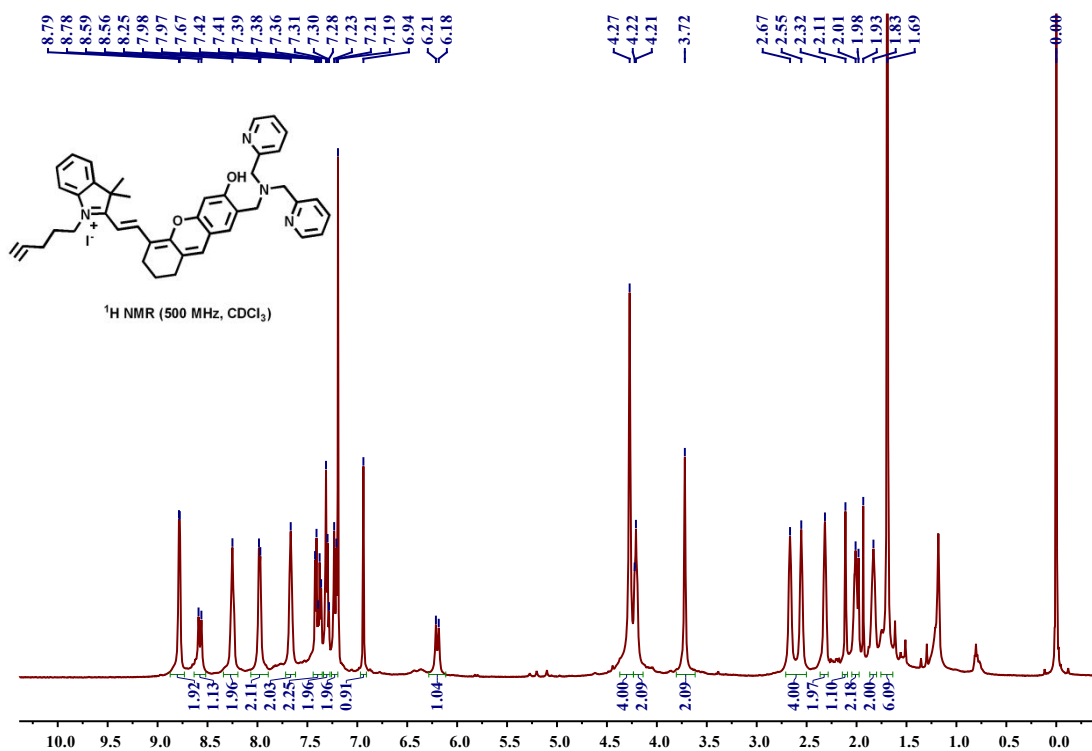


Figure S23. ¹H NMR spectrum of compound **Hd-BPA** in CDCl₃.

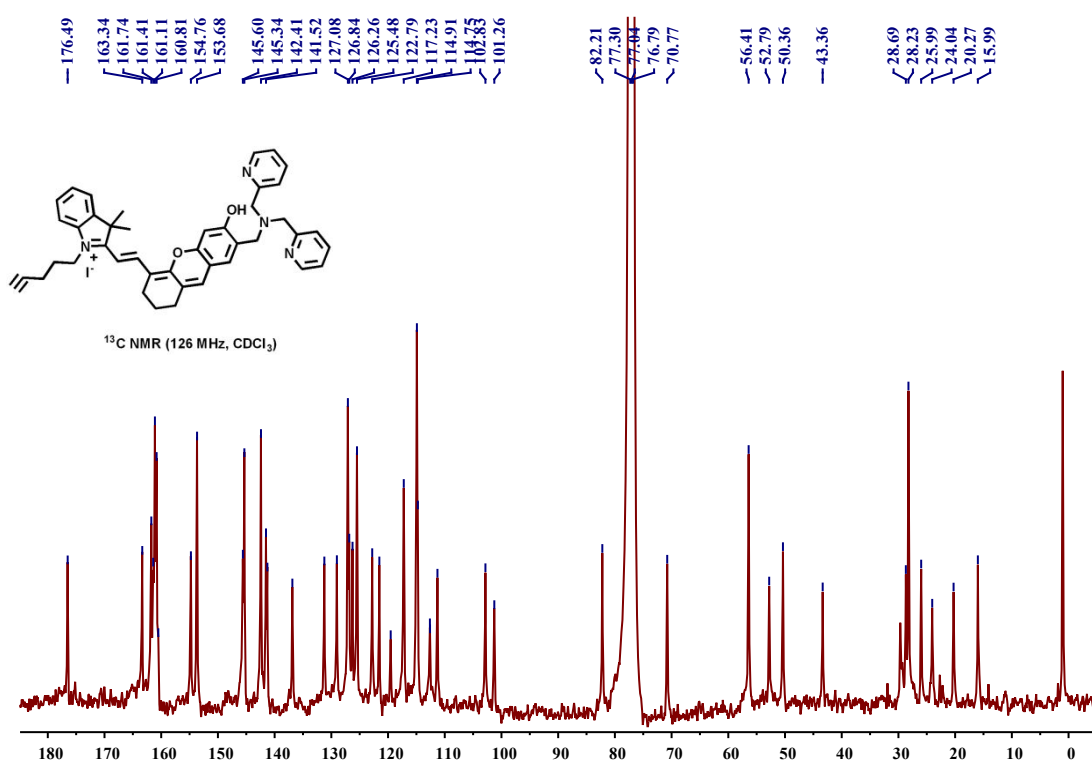


Figure S24. ¹³C NMR spectrum of compound **Hd-BPA** in CDCl₃.

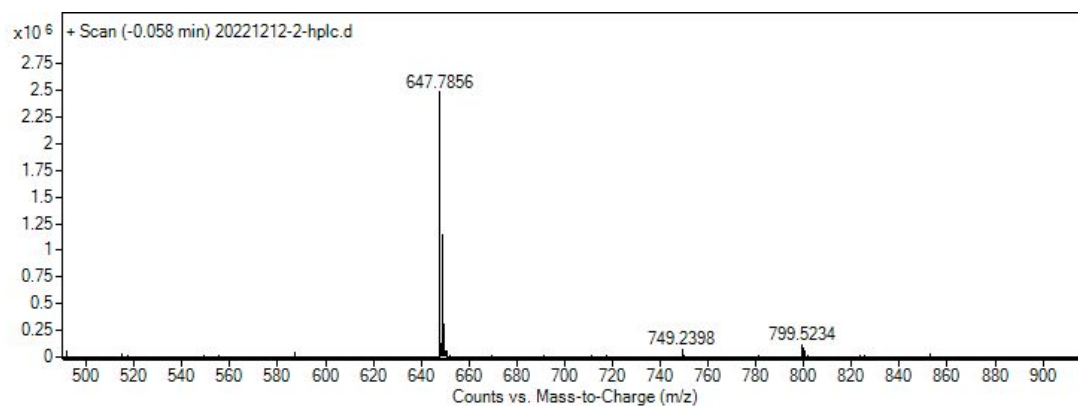


Figure S25. HRMS spectrum of compound **Hd-BPA**.

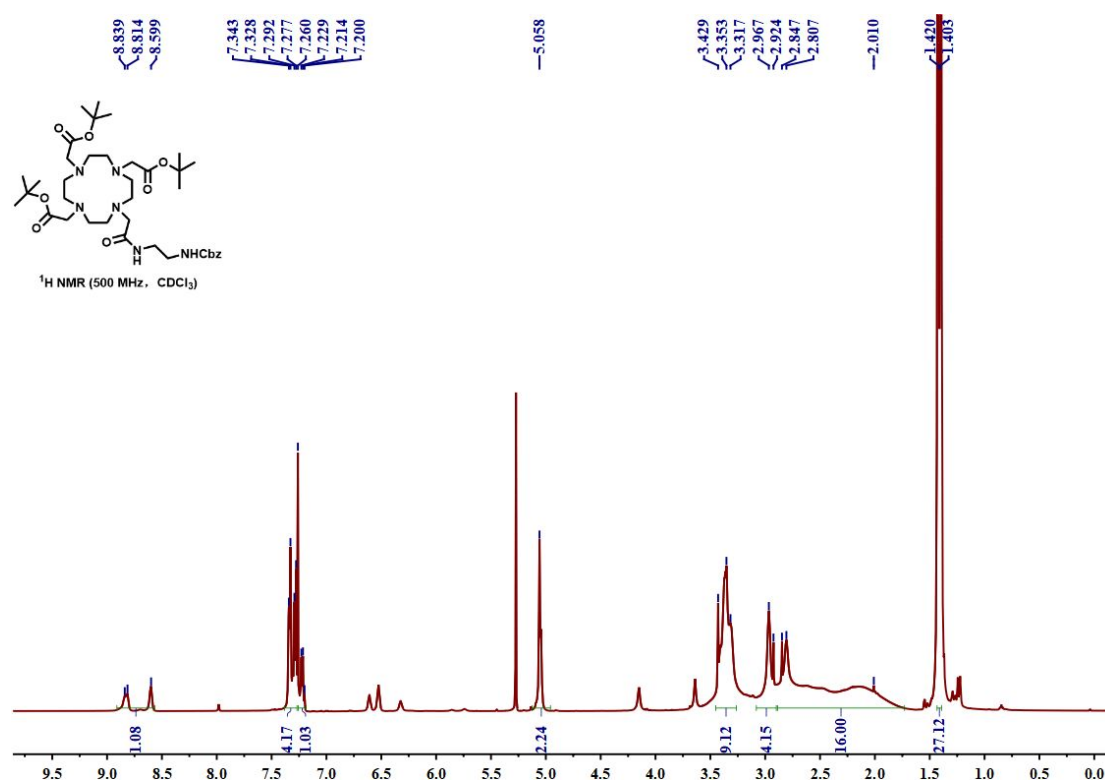


Figure S26. ¹H NMR spectrum of compound **1** in CDCl₃.

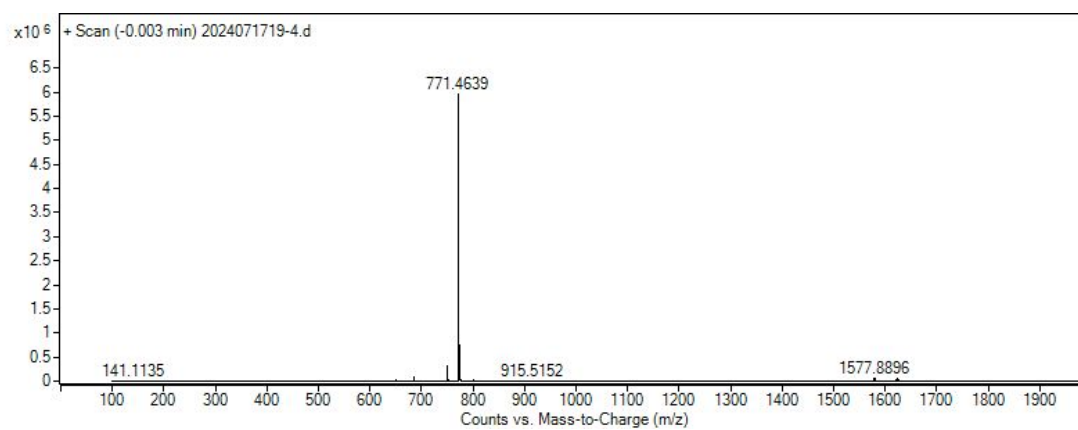


Figure S27. HRMS spectrum of compound **1**.

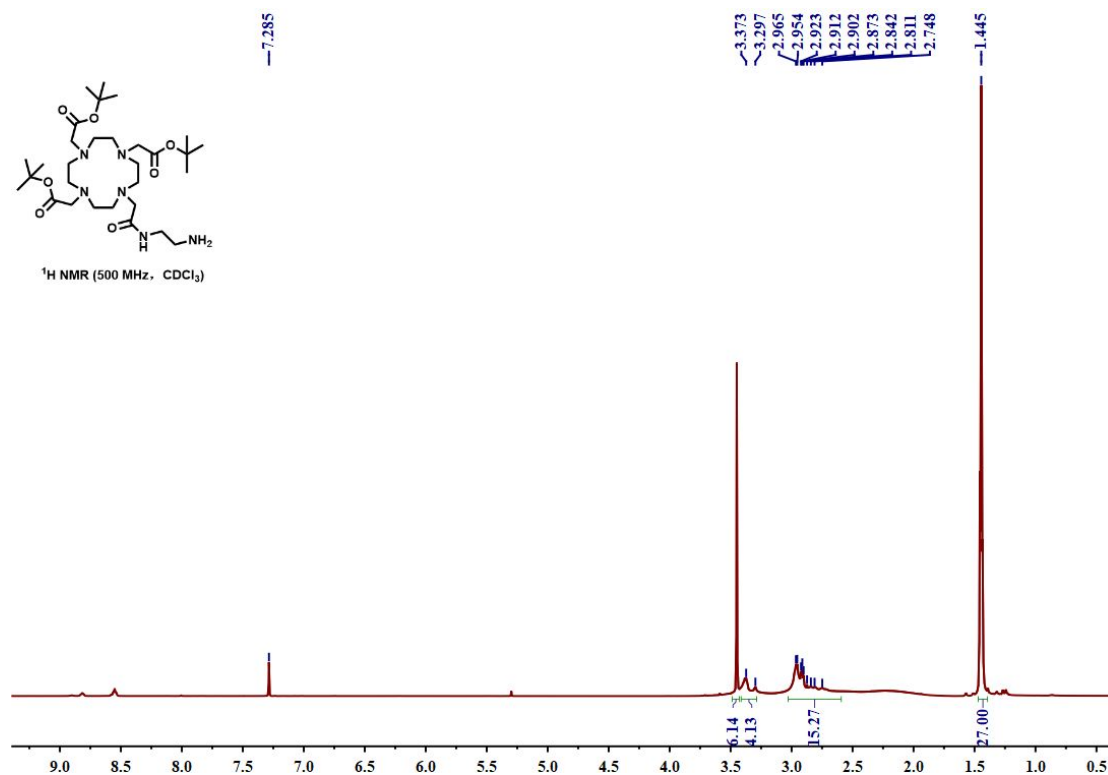


Figure S28. ¹H NMR spectrum of compound **2** in CDCl₃.

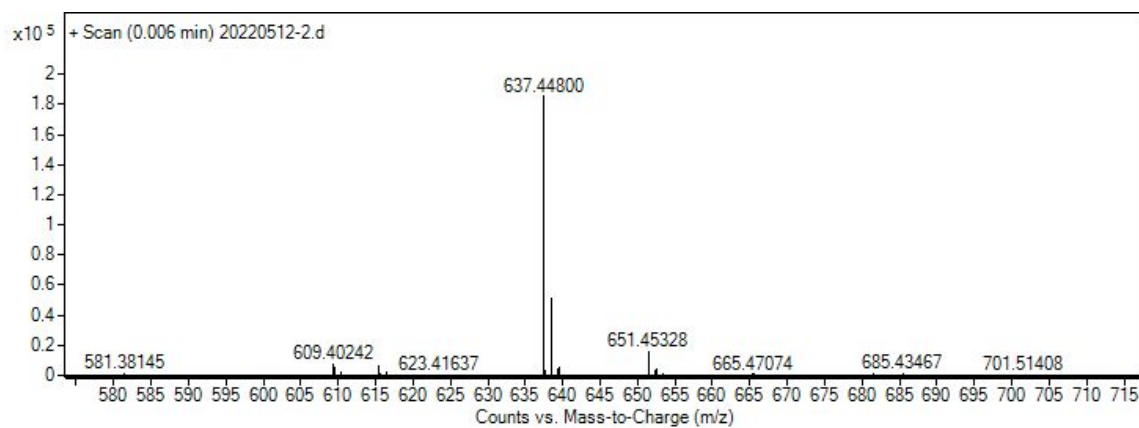


Figure S29. HRMS spectrum of compound **2**.

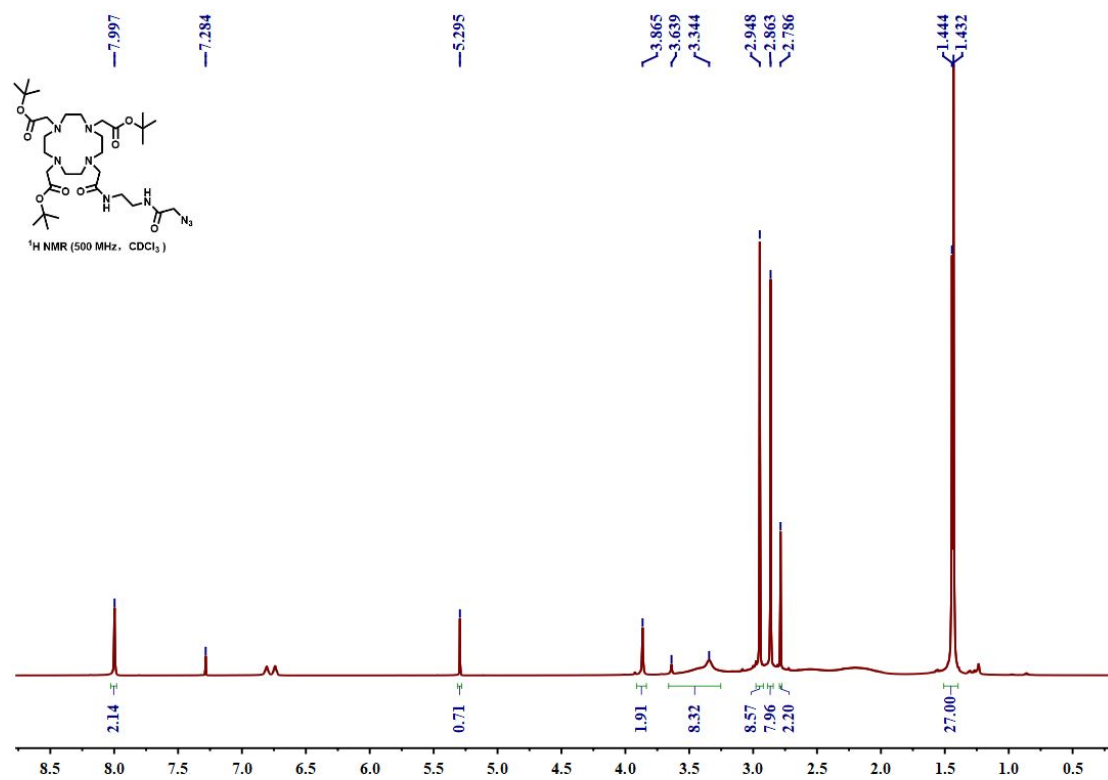


Figure S30. ¹H NMR spectrum of compound **3** in CDCl₃.

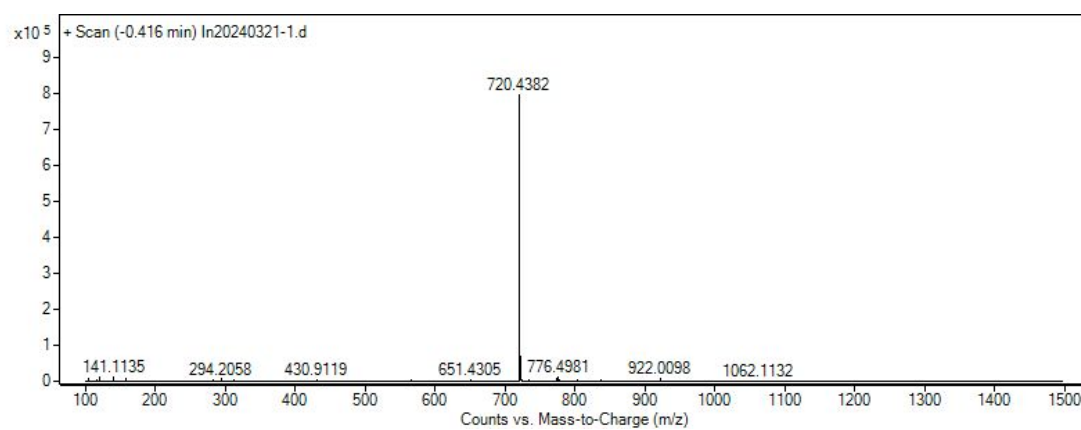


Figure S31. HRMS spectrum of compound **3**.